Comparisons between Classical, Semiclassical, and Quantum Plasmonics in Graphene Nanodisks

Thomas Christensen,[1,2,*] Weihua Wang,[1,2,*] Martijn Wubs,[1,2] Antti-Pekka Jauho,[2,3] and N. Asger Mortensen[1,2]

[1]*Department of Photonics Engineering, Technical University of Denmark, DK-2800 Kgs. Lyngby, Denmark*
[2]*Center for Nanostructured Graphene, Technical University of Denmark, DK-2800 Kgs. Lyngby, Denmark*
[3]*Department of Micro- and Nanotechnology, Technical University of Denmark, DK-2800 Kgs. Lyngby, Denmark*

We study the transitions from classical, semiclassical, and quantum plasmonic behavior in graphene nanodisks in the quasistatic limit. Specifically, we investigate four hierarchies of approximation: **1.** Local-reponse approximation (LRA), embodying the traditional approach in plasmonic light-matter interaction. **2.** Hydrodynamic response, adapted to the response of graphene, including the first nonlocal correction to its optical response. **3.** Real-space random phase approximation (RPA) formulation with electron states calculated from the Dirac-Weyl equation, with infinite mass and zigzag boundary conditions (BCs). **4.** Real-space RPA with electron states calculated from a nearest-neighbor tight-binding (TB) treatment. See Figure 1 for a summary of the considered hierarchies.

Levels 1 and 2 constitute bulk response approximations, while levels 3 and 4 take the finite extent of the graphene structure into consideration with different precision: in the Dirac-Weyl treatment, the Hamiltonian is that of bulk graphene in the low-energy regime with boundary conditions accounting approximately for the topology and extent of the structure, whilst the TB treatment accounts naturally for the atomistic features of the structure. Additionally, levels 3 and 4 also naturally include the effects of energy level quantization and nonlocality.

Graphene nanodisks are considered, which allows semi-analytical treatments for approaches 1 through 3. Additionally, nanodisks, with their nontrivial edge-configurations, highlight the importance of edge states in TB treatments. The treatment of edge-states is completely absent in the bulk descriptions, i.e. in the LRA and hydrodynamics, but can be qualitatively accounted for in the Dirac-Weyl approach with zigzag BCs.

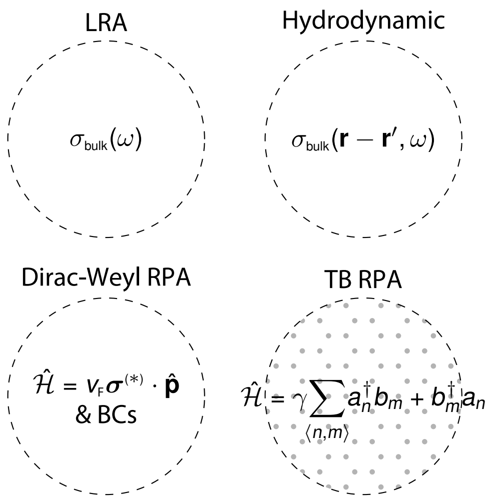

FIG. 1: Schematic illustration of the considered levels of approximation in our treatment.

Below we explicate the essence of the four approaches:

1. Local-response approximation: Taking the local-response limit of the low-energy dispersion $\epsilon = \pm\hbar v_{\text{F}} k$ response result, the conductivity of graphene is given by:[1]

$$\sigma_{\text{bulk}}(\omega) = \sigma_{\text{D}}(\omega) + \sigma_{\text{I}}(\omega), \tag{1}$$

with intra- (Drude) and inter-band contributions

$$\sigma_{\text{D}}(\omega) = \frac{ie^2\epsilon_{\text{F}}}{\pi\hbar(\omega+i\gamma)}, \quad \sigma_{\text{I}}(\omega) = \frac{ie^2}{4\pi\hbar}\log\left|\frac{2\epsilon_{\text{F}}-\hbar\omega}{2\epsilon_{\text{F}}+\hbar\omega}\right|.$$

with Fermi level ϵ_{F} and loss rate γ.

2. Hydrodynamic reponse in graphene: A Taylor approximation of the low-energy response result to first non-vanishing component in momentum, k, yields (neglecting loss):

$$\sigma(k,\omega) \simeq \sigma_{\text{D}}(\omega)\left(1+\frac{\beta_{\text{D}}^2}{\omega^2}k^2\right) + \sigma_{\text{I}}(\omega)\left(1+\frac{\beta_{\text{I}}^2}{\omega^2}k^2\right), \tag{2}$$

where the plasma velocities $\beta_{\text{D}} = \sqrt{3/4}v_{\text{F}}$ and $\beta_{\text{I}} = \sqrt{1/2}v_{\text{F}}$ differ. Neglecting this difference and letting $\beta_{\text{I}} \to \beta_{\text{D}}$, which induces only a small error since the Drude contribution is usually dominant, allows recasting the response as a single hydrodynamic equation for the current $\mathbf{J}$ and electric field $\mathbf{E}$:

$$\mathbf{J}(\mathbf{r},\omega) + \frac{\beta_{\text{D}}^2}{\omega^2}\nabla_{\parallel}\left[\nabla_{\parallel}\cdot\mathbf{J}(\mathbf{r},\omega)\right] = \sigma_{\text{D}}(\omega)\mathbf{E}(\mathbf{r},\omega). \tag{3}$$

In both hydrodynamic and local descriptions we solve the electrostatic problem due to an incident wave using a semi-analytical polynomial expansion technique.[2]

3. Dirac-Weyl and RPA: The Dirac-Weyl equation for uncoupled Dirac valleys can be cast as a two-spinor equation $\hat{\mathcal{H}}\psi = \epsilon\psi$ with the Hamiltonian $\hat{\mathcal{H}}^{K} = v_{\text{F}}\boldsymbol{\sigma}\cdot\hat{\mathbf{p}}$ for the $\mathbf{K}$-valley (and $\hat{\mathcal{H}} = v_{\text{F}}\boldsymbol{\sigma}^*\cdot\hat{\mathbf{p}}$ for the $\mathbf{K}'$ valley), and spinor components associated with the A- and B-sublattice.[3] BCs corresponding to zigzag, armchair, and mass confinement can be imposed. Here we focus on the comparison of zigzag[4] and mass confinement.[5] Application of BCs discretizes the allowed states $\{\epsilon, \psi\}_{ln}$ with angular and radial quantum numbers l and n. Additionally, an infinitely degenerate band of zero-energy edge-states exist for the zigzag BC.

The non-interacting polarizability, χ^0, is computed in a real-space formulation according to:[6]

$$\chi^0(\mathbf{r}, \mathbf{r}'; \omega) = 2 \sum_{\kappa l l' n n'} \frac{f^\kappa_{l'n'} - f^\kappa_{ln}}{\hbar\omega + i\hbar\eta - (\epsilon^\kappa_{ln} - \epsilon^\kappa_{l'n'})} \times [\psi^{\kappa\dagger}_{l'n'}(\mathbf{r})\psi^{\kappa\dagger}_{ln}(\mathbf{r})][\psi^{\kappa\dagger}_{ln}(\mathbf{r}')\psi^{\kappa}_{l'n'}(\mathbf{r}')], \tag{4}$$

with the summation extending also over the valley index κ, with Fermi-Dirac functions f^κ_{ln}, and with electron relaxation-rate $\eta = \gamma/2$.

4. Tight-binding and RPA: The TB Hamiltonian, including only nearest-neighbor interaction with energy γ, reads as $\hat{\mathcal{H}} = \gamma \sum_{\langle j,j' \rangle} \hat{a}_j^\dagger \hat{b}_{j'} + \hat{b}_{j'}^\dagger \hat{a}_j$, with A- and B-sublattice annihilation (creation) operators $\hat{a}_j^{(\dagger)}$ and $\hat{b}_j^{(\dagger)}$ for 2p orbitals at site j and position $\mathbf{r}_j$. Diagonalization of this Hamiltonian yields the electron states. The polarizability is evaluable at the lattice sites, i.e. it takes a discrete representation in real-space $\chi^0(\mathbf{r}_j, \mathbf{r}_{j'}; \omega)$. It is determined following the scheme in Eq. (4), but with the summation running over the TB states.[6]

The interaction with external potentials ϕ^{ext}, for both the Dirac-Weyl and TB approaches, is introduced by self-consistently coupling the total potential ϕ and the induced charge ρ through the equations $\rho(\mathbf{r}) = \int \chi^0(\mathbf{r}, \mathbf{r}')\phi(\mathbf{r}')\,\mathrm{d}\mathbf{r}'$ and $\phi(\mathbf{r}) = \phi^{\mathrm{ext}}(\mathbf{r}) + \int V(\mathbf{r}, \mathbf{r}')\rho(\mathbf{r}')\,\mathrm{d}\mathbf{r}'$, with $V(\mathbf{r}, \mathbf{r}')$ denoting the Coulomb interaction, thereby applying the RPA.

In our comparison of the above four approaches for graphene nanodisks we examine and focus on the following aspects: **(a)** The emergence of nonclassical features in the optical response of nanodisks at small radii, being distinct but qualitatively similar in the Dirac-Weyl and TB approaches. These features are due in part to near-zero energy edge states and in part due to energy level quantization. **(b)** Assessing the role of nonlocality in the optical response. We find excellent agreement between the Dirac-Weyl and hydrodynamic approaches at larger radii, both exhibiting quantitatively identical blueshifts compared with the LRA result. These predictions of blueshifts, however, stand in contrast with the predictions of TB which predict minor redshifts[6] of the dipole resonance. **(c)** The sensitivity of TB calculations to atomistic configuration variations, for fixed radii, and sensitivity to polarization-angle. We consider the ensemble-averaging of TB optical spectra and compare with the continuum approaches.

We hope that our comparisons of the different hierarchies of approximation will offer new insight into the nature of quantum plasmonic effects in graphene nanostructures. Additionally, we aim to showcase the applicability of the continuum Dirac-Weyl approach, and the feasibility of including the effects of nonlocality and energy quantization in a single continuum scheme. In geometries with well-defined edges, such as zigzag or armchair, we predict that the Dirac-Weyl approach will generally agree very well with TB calculations, but at a reduced numerical cost and with a more transparent interpretation.

Acknowledgments

The Center for Nanostructured Graphene is sponsored by the Danish National Research Foundation, Project DNRF58. This work was also supported by the Danish Council for Independent Research - Natural Sciences, Project 1323-00087.

* T. Christensen and W. Wang contributed equally to this work.

1 L. A. Falkovsky and A. A. Varlamov, Eur. Phys. J. B **56**, 281 (2007).
2 A. Fetter, Phys. Rev. B **33**, 5221 (1986).
3 A. Castro Neto, F. Guinea, N. Peres, K. Novoselov, and A. Geim, Rev. Mod. Phys. **81**, 109 (2009).
4 L. Brey and H. Fertig, Phys. Rev. B **73**, 195408 (2006).
5 M. Berry and R. Mondragon, Proc. R. Soc. Lond. A **412**, 53 (1987).
6 S. Thongrattanasiri, A. Majavacas, and F. García de Abajo, ACS Nano **6**, 1766 (2012).